Journal of the American College of Cardiology
© 2014 by the American College of Cardiology Foundation
Published by Elsevier Inc.

Vol. 63, No. 6, 2014
ISSN 0735-1097/$36.00
http://dx.doi.org/10.1016/j.jacc.2013.10.062

Coxsackie and Adenovirus Receptor Is a Modifier of Cardiac Conduction and Arrhythmia Vulnerability in the Setting of Myocardial Ischemia

Roos F. J. Marsman, MSc,* Connie R. Bezzina, PhD,* Fabian Freiberg, MSc,† Arie O. Verkerk, PhD,‡ Michiel E. Adriaens, PhD,* Svitlana Podliesna, MSc,* Chen Chen, PhD,† Bettina Purfürst, PhD,§ Bastian Spallek, DVM,‖ Tamara T. Koopmann, PhD,* Istvan Baczko, MD, PhD,¶ Cristobal G. dos Remedios, PhD,# Alfred L. George, Jr, MD,** Nanette H. Bishopric, MD,†† Elisabeth M. Lodder, PhD,* Jacques M. T. de Bakker, PhD,*‡‡ Robert Fischer, MD,‖ Ruben Coronel, MD, PhD,* Arthur A. M. Wilde, MD, PhD,* Michael Gotthardt, MD,†§§ Carol Ann Remme, MD, PhD*

Amsterdam and Utrecht, the Netherlands; Berlin-Buch and Berlin, Germany; Szeged, Hungary; Sydney, Australia; Nashville, Tennessee; and Miami, Florida

Objectives The aim of this study was to investigate the modulatory effect of the coxsackie and adenovirus receptor (CAR) on ventricular conduction and arrhythmia vulnerability in the setting of myocardial ischemia.

Background A heritable component in the risk of ventricular fibrillation during myocardial infarction has been well established. A recent genome-wide association study of ventricular fibrillation during acute myocardial infarction led to the identification of a locus on chromosome 21q21 (rs2824292) in the vicinity of the *CXADR* gene. CXADR encodes the CAR, a cell adhesion molecule predominantly located at the intercalated disks of the cardiomyocyte.

Methods The correlation between CAR transcript levels and rs2824292 genotype was investigated in human left ventricular samples. Electrophysiological studies and molecular analyses were performed using CAR haploinsufficient ($CAR^{+/-}$) mice.

Results In human left ventricular samples, the risk allele at the chr21q21 genome-wide association study locus was associated with lower *CXADR* messenger ribonucleic acid levels, suggesting that decreased cardiac levels of CAR predispose to ischemia-induced ventricular fibrillation. Hearts from $CAR^{+/-}$ mice displayed slowing of ventricular conduction in addition to an earlier onset of ventricular arrhythmias during the early phase of acute myocardial ischemia after ligation of the left anterior descending artery. Expression and distribution of connexin 43 were unaffected, but $CAR^{+/-}$ hearts displayed increased arrhythmia susceptibility on pharmacological electrical uncoupling. Patch-clamp analysis of isolated $CAR^{+/-}$ myocytes showed reduced sodium current magnitude specifically at the intercalated disk. Moreover, CAR coprecipitated with $Na_V1.5$ in vitro, suggesting that CAR affects sodium channel function through a physical interaction with $Na_V1.5$.

Conclusions CAR is a novel modifier of ventricular conduction and arrhythmia vulnerability in the setting of myocardial ischemia. Genetic determinants of arrhythmia susceptibility (such as CAR) may constitute future targets for risk stratification of potentially lethal ventricular arrhythmias in patients with coronary artery disease. (J Am Coll Cardiol 2014;63:549–59) © 2014 by the American College of Cardiology Foundation

From the *Heart Failure Research Center, Department of Clinical and Experimental Cardiology, Academic Medical Center, Amsterdam, the Netherlands; †Neuromuscular and Cardiovascular Cell Biology, Max Delbrück Center for Molecular Medicine, Berlin-Buch, Germany; ‡Heart Failure Research Center, Department of Anatomy, Embryology and Physiology, Academic Medical Center, Amsterdam, the Netherlands; §Electron Microscopy Core Facility, Max Delbrück Center for Molecular Medicine, Berlin, Germany; ‖Universitätsklinikum Benjamin Franklin, Charité, University Medicine Berlin, Berlin, Germany; ¶Department of Pharmacology and Pharmacotherapy, University of Szeged, Szeged, Hungary; #Muscle Research Unit, Institute for Biomedical Research, University of Sydney, Sydney, Australia; **Division of Genetic Medicine, Department of Medicine, Vanderbilt University, Nashville, Tennessee; ††University of Miami Cardiovascular Genomics Laboratory, University of Miami Miller School of Medicine, Miami, Florida; ‡‡Interuniversity Cardiology Institute of the Netherlands, Utrecht, the Netherlands; and the §§DZHK (German Centre for

JACC Vol. 63, No. 6, 2014
February 18, 2014:549–59

Abbreviations and Acronyms

AP = action potential
CAR = coxsackie and adenovirus receptor
CVL = longitudinal conduction velocity
CVT = transversal conduction velocity
Cx = connexin
GWAS = genome-wide association study
I_{Na} = sodium current
LAD = left anterior descending
MI = myocardial infarction
mRNA = messenger ribonucleic acid
VF = ventricular fibrillation
VT = ventricular tachycardia
WT = wild-type

Ventricular fibrillation (VF) is a frequent and potentially lethal complication of acute myocardial infarction (MI). In this setting, VF is the consequence of disturbed electrical properties of the ischemic myocardium, which includes a decrease in cardiomyocyte excitability and cell-to-cell coupling. These factors result in conduction slowing of the cardiac electrical impulse, which is a prerequisite for the occurrence of life-threatening arrhythmias such as VF in MI (1).

See page 560

Traditional cardiovascular risk factors do not identify which patient with MI is at risk for VF, and specific and sensitive risk predictors are currently lacking. A heritable component in the determination of risk of VF and sudden cardiac death during MI has been well established (2,3), but progress in understanding the molecular and genetic determinants of ischemia-induced VF has been limited. To identify susceptibility genes, our group recently conducted a genome-wide association study (GWAS) that led to the identification of common genetic variants at the chromosome 21q21 locus associated with the risk of VF in the setting of acute MI (4). The most significant association signal for VF on the chromosome 21q21 locus comprised the single nucleotide polymorphism rs2824292, located immediately upstream of 2 genes, *CXADR* and *BTG3* (the only genes within a region of 1 megabase spanning the association signal) (4). The *BTG3* gene encodes B-cell translocation gene 3, a member of the antiproliferative BTG/Tob protein family, known to regulate cell cycle progression, gene expression, tumorigenesis, and cancer (5). The *CXADR* gene encodes the coxsackie and adenovirus receptor (CAR), a transmembrane cell adhesion molecule predominantly located at the intercalated disk between cardiomyocytes (6–9). CAR has been recognized primarily for its involvement in virus-mediated myocarditis, but recent studies in CAR knockout mice revealed atrioventricular conduction slowing due to loss of expression of the gap junction protein connexin (Cx) 45 (9,10). Moreover, expression levels of Cx43, the predominant gap junction molecule in ventricular myocardium, were decreased in hearts from CAR knockout mice (9), raising the possibility that CAR may play a role in ventricular conduction. Of note, CAR is known to be differentially regulated in various cardiac disease states, including dilated cardiomyopathy and MI (6,11).

We hypothesized that CAR affects ventricular conduction and susceptibility to ventricular arrhythmia in the setting of MI and show that the rs2824292 risk genotype is associated with decreased expression of *CXADR* in the human heart. Furthermore, we show that mice haploinsufficient for CAR display ventricular conduction slowing and an earlier onset of ventricular arrhythmias during MI, at least in part mediated by a reduced sodium current (I_{Na}) magnitude at the intercalated disk.

Methods

The methods are provided in the Online Appendix.

Results

rs2824292 regulates cardiac expression of *CXADR*, the gene encoding CAR. Because the risk haplotype tagged by rs2824292 occurs in a noncoding region of chr21q21, it is likely to affect the risk of VF through effects on gene expression. We therefore investigated whether the rs2824292 genotype correlates to transcript expression levels of the only 2 neighboring genes within 1 megabase, namely *CXADR* (located 100 kilobases downstream of rs2824292) and *BTG3* (located 179 kilobases downstream). Assessment of transcript abundance for these genes in normal donor heart myocardium (n = 129) uncovered an association between the genotype at rs2824292 and cardiac *CXADR* messenger ribonucleic acid (mRNA) levels (Fig. 1). Subjects carrying 1 or 2 copies of the risk allele (AG or GG genotype) displayed significantly lower (0.6-fold) *CXADR* mRNA expression compared with subjects with the nonrisk (AA) genotype (dominant model: $p = 0.002$; additive model: $p = 0.006$). No such relationship was observed with cardiac expression of *BTG3*. Thus, the VF risk allele at rs2824292 is associated with decreased cardiac expression of *CXADR*, suggesting that decreased levels of CAR predispose to VF during ischemia.

CAR haploinsufficient mice. To investigate the effects of reduced CAR expression on cardiac conduction and arrhythmogenesis, we generated mice deficient for CAR (Online Fig. 1) (12). Homozygous CAR-deficient mice were not viable and died midgestation between embryonic days 10.5 and 12.5 (Online Fig. 2, Online Table 1). Heterozygous CAR-deficient mice ($CAR^{+/-}$) were born at the expected Mendelian ratio (Online Table 1) and had a normal life span.

Cardiovascular Research), partner site, Berlin, Germany. This study was supported by the Netherlands Heart Foundation (2005T025, 2007B010, 2010B175), the Deutsche Forschungsgemeinschaft (to Dr. Gotthardt), the National Institutes of Health (grant HL068880 to Dr. George), the Netherlands Heart Institute (ICIN 061.02), and the Division for Earth and Life Sciences (project 836.09.003 to Dr. Remme), with financial aid from the Netherlands Organization for Scientific Research. This research was performed within the framework of the Center for Translational Molecular Medicine, project COHFAR (grant 01C-203). Dr. Wilde is a member of the scientific advisory board for Sorin. All other authors have reported that they have no relationships relevant to the content of this paper to disclose.

Manuscript received June 30, 2013; revised manuscript received October 13, 2013, accepted October 22, 2013.

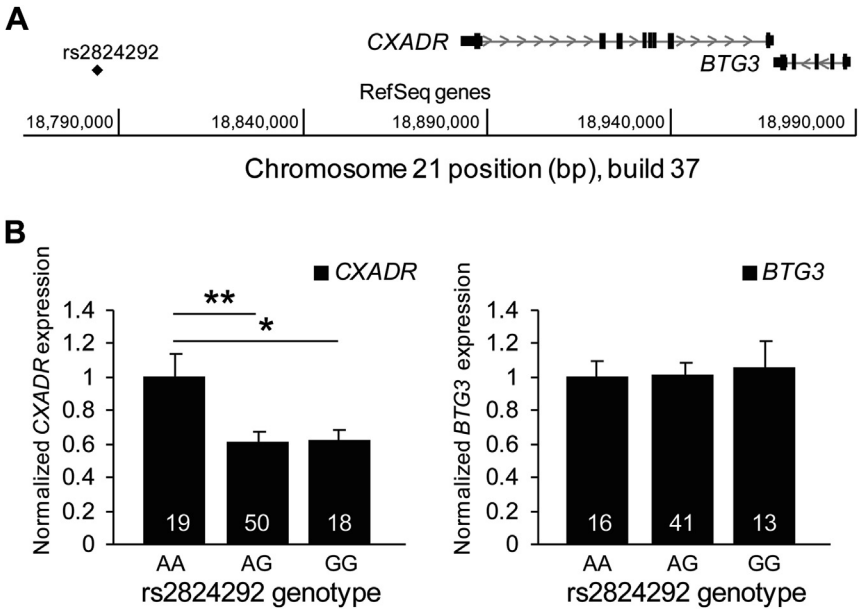

Figure 1 **rs2824292 Regulates Cardiac *CXADR* Levels**

(A) The human 21q21 locus. *CXADR* and *BTG3* are located within a 500-kilobase region downstream of rs2824292. **(B)** Mean mRNA expression of *CXADR* and *BTG3* as a function of genotype at rs2824292 in human heart samples, standardized to the geomean of *cTNI* and *HPRT* mRNA expression levels (*p = 0.05; **p < 0.01). Mean expression levels in hearts from AG heterozygotes and GG homozygotes are normalized to the mean expression levels from hearts of AA homozygotes. bp = base pairs; mRNA = messenger ribonucleic acid.

Earlier onset of inducible ventricular arrhythmias during acute myocardial ischemia in CAR$^{+/-}$ mouse hearts. To investigate whether reduced CAR levels predispose to arrhythmia during acute myocardial ischemia, we induced regional ischemia in Langendorff-perfused wild-type (WT) and CAR$^{+/-}$ hearts by ligating the left anterior descending (LAD) artery and tested arrhythmia inducibility. Ischemic zone size was not significantly different between WT and CAR$^{+/-}$ hearts (Fig. 2A). Hearts were stimulated from the nonischemic area at a basic cycle length of 120 ms (S1), and arrhythmia inducibility was tested before ligation of the LAD artery and at different intervals during ischemia using up to 3 extrastimuli (S2-S3-S4) and burst pacing. Spontaneous sustained arrhythmias did not occur in WT or CAR$^{+/-}$ hearts at baseline or during the ischemic period. Arrhythmias were never induced before ligation of the LAD artery but were induced in all WT and CAR$^{+/-}$ hearts during ischemia. These included premature ventricular contractions, nonsustained ventricular tachycardia (VT), and sustained VT (Fig. 2B). During the first 15 min of ischemia, we observed inducible arrhythmias (nonsustained and sustained) in 7 of 9 CAR$^{+/-}$ hearts. In contrast, arrhythmias were induced in only 1 of 8 WT hearts ($p < 0.05$) (Figs. 2C and 2D). Similarly, in the first 15 min of ischemia, there was a trend toward a higher prevalence of inducible sustained VT (>3 s) in CAR$^{+/-}$ compared with WT hearts (Fig. 2E). During later stages of the ischemic episode, arrhythmia inducibility was not different between WT and CAR$^{+/-}$ hearts. Thus, CAR$^{+/-}$ hearts displayed an advanced onset of ventricular arrhythmia inducibility during the early phase of acute myocardial ischemia.

Ventricular conduction slowing in isolated CAR$^{+/-}$ hearts. We hypothesized that altered electrophysiological properties secondary to CAR deficiency render CAR$^{+/-}$ hearts more susceptible to arrhythmia inducibility in the setting of myocardial ischemia. Surface electrocardiographic analysis showed no significant differences in electrocardiographic parameters (RR, PQ, QRS, and QTc intervals) between CAR$^{+/-}$ and WT mice (Online Fig. 3). We therefore studied ventricular conduction in more detail by electrical mapping of isolated WT and CAR$^{+/-}$ hearts. A 247-point electrode was placed on the left ventricular epicardial surface, and hearts were stimulated from the center of the electrode. Local electrograms were used to construct activation maps (Fig. 3A), from which longitudinal conduction velocity (CVL) and transversal conduction velocity (CVT) were determined. The stimulation threshold and shortest coupled intervals of S2, S3, and S4 (effective refractory period) were not significantly different between CAR$^{+/-}$ and WT hearts (Online Table 3). During basic stimulation (S1), CVL (CAR$^{+/-}$: 63.7 ± 4.7 cm/s; WT: 77.8 ± 2.8 cm/s; $p = 0.02$) and CVT (CAR$^{+/-}$: 28.6 ± 2.0 cm/s; WT: 38.0 ± 2.5 cm/s; $p = 0.01$) were significantly reduced in CAR$^{+/-}$ compared with WT hearts (Figs. 3B and 3C). These differences in conduction velocity were also observed after application of 3 extrastimuli (S4; CAR$^{+/-}$:

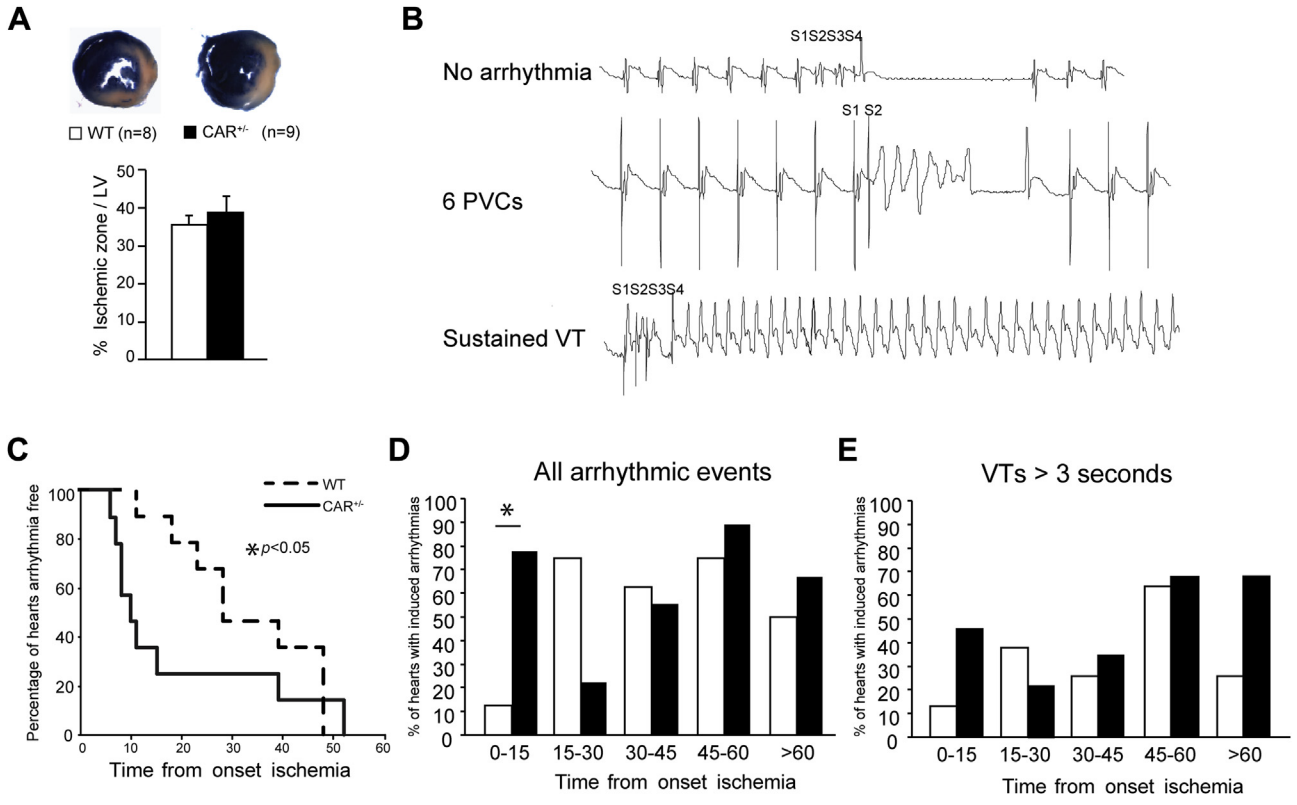

Figure 2 **Accelerated Onset of Inducible Arrhythmias During Myocardial Ischemia in Isolated CAR$^{+/-}$ Hearts**

(A) Ischemic zone size after ligation of the LAD artery (nonperfused area; as a percentage of the left ventricle) was similar in WT and CAR$^{+/-}$ hearts. **(B)** Arrhythmia inducibility during ligation of the LAD artery. Typical examples of ventricular electrograms show extrastimuli (S1 to S4) followed by either arrhythmia **(upper panel)**, 6 ventricular extrasystoles (PVCs) **(middle panel)**, or sustained VT **(lower panel)**. **(C)** Kaplan-Meier plot showing an accelerated onset of first arrhythmic event during myocardial ischemia in CAR$^{+/-}$ hearts (n = 9) as compared with WT (n = 8). **(D and E)** CAR$^{+/-}$ hearts display increased inducibility of **(D)** all types of arrhythmia and **(E)** sustained VT (>3 s) during the first 15 min of ischemia (*p < 0.05). CAR = coxsackie and adenovirus receptor; LAD = left anterior descending; LV = left ventricular; PVC = premature ventricular contraction; VT = ventricular tachycardia; WT = wild-type.

42.5 ± 4.6 cm/s; WT: 55.5 ± 4.2 cm/s; p = 0.054) and CVT (CAR$^{+/-}$: 28.6 ± 1.8 cm/s; WT: 33.9 ± 1.5 cm/s; p = 0.04) (Figs. 3B and 3C).

Pharmacological electrical uncoupling induces ventricular arrhythmias in CAR$^{+/-}$ hearts. Conduction slowing in CAR$^{+/-}$ hearts may stem from altered tissue architecture, cell-to-cell coupling, and/or cardiomyocyte excitability. No evidence for myocardial hypertrophy or fibrosis was found in CAR$^{+/-}$ hearts (Online Fig. 4). In addition, transmission electron microscopy did not reveal ultrastructural changes in CAR$^{+/-}$ hearts (Online Fig. 5). To evaluate whether the conduction slowing in CAR$^{+/-}$ hearts is mediated by alterations in gap junction composition and/or function, we investigated the expression and distribution of connexins and challenged WT and CAR$^{+/-}$ hearts with the gap junction uncoupler carbenoxolone. Carbenoxolone is known to decrease conduction velocity both in the longitudinal and transversal direction without affecting action potential (AP) characteristics and underlying ionic currents (13). During stimulation at basic cycle length (S1), carbenoxolone significantly reduced CVL in both WT and CAR$^{+/-}$ hearts (Fig. 3B). Similarly, CVT was decreased by carbenoxolone in WT and CAR$^{+/-}$ hearts after application of 3 extrastimuli (S4) (Fig. 3C).

The consequences of the observed conduction slowing after infusion of carbenoxolone with respect to arrhythmia inducibility were tested using up to 3 extrastimuli (S2-S3-S4) and burst pacing. The shortest possible coupling intervals of S2-S3-S4 and burst trains were not significantly different between CAR$^{+/-}$ and WT hearts at baseline and after infusion of carbenoxolone (Online Table 3). Spontaneous arrhythmias did not occur in either experimental group, and we were unable to induce arrhythmias in WT or CAR$^{+/-}$ hearts at baseline. Although none of the WT hearts showed induced arrhythmias on infusion of carbenoxolone, 50% of the CAR$^{+/-}$ hearts developed sustained ventricular arrhythmias during burst pacing after administration of carbenoxolone (CAR$^{+/-}$: 4/8; WT: 0/9; p = 0.015) (Figs. 4A and 4B). VTs induced in CAR$^{+/-}$ hearts after infusion of carbenoxolone were reproducible

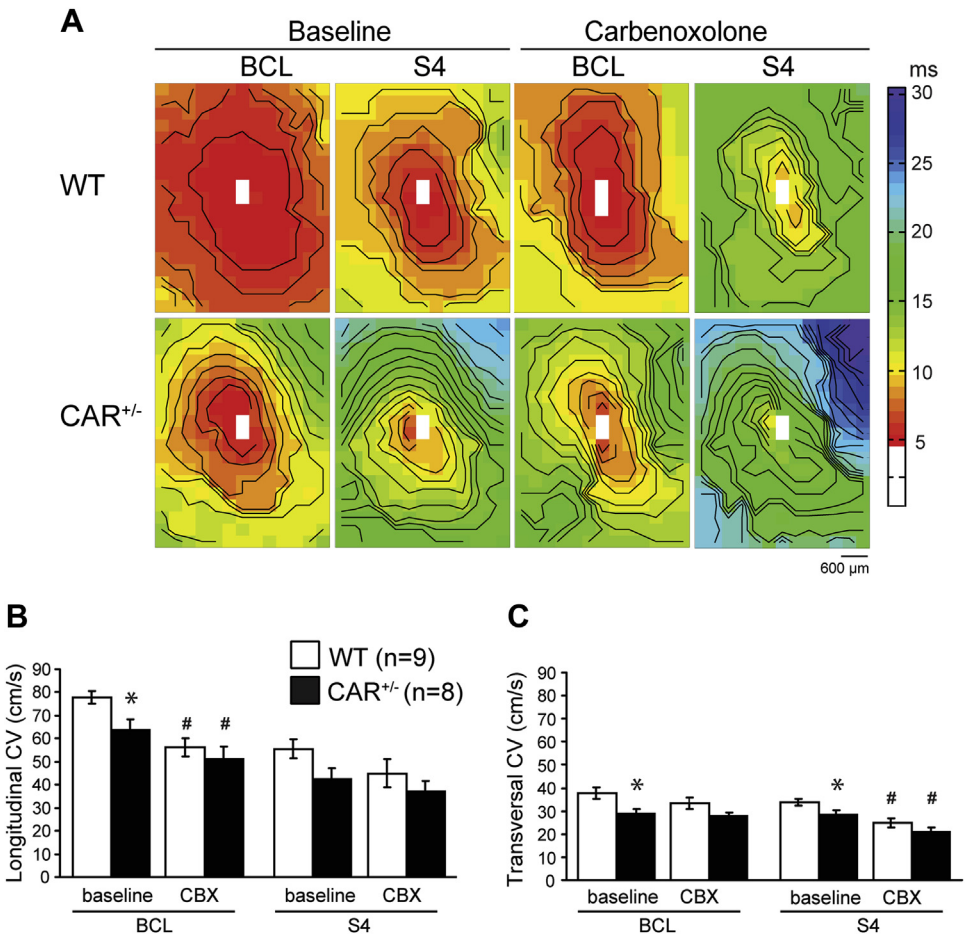

Figure 3 **Ventricular Conduction Slowing in CAR$^{+/-}$ Hearts**

(A) Representative left ventricular epicardial activation maps at baseline and after infusion of CBX in WT and CAR$^{+/-}$ hearts. Crowding of isochrones is indicative of conduction slowing. Average **(B)** longitudinal and **(C)** transversal conduction velocities measured during basic stimulation (120 ms) and 3 extrastimuli (S4) at baseline and after administration of CBX (*$p < 0.05$ CAR$^{+/-}$ vs. WT; #$p < 0.05$ CBX vs. baseline). BCL = basic cycle length (120 ms); CBX = carbenoxolone; other abbreviations as in Figure 2.

and lasted for more than 5 s to 1 min. Activation maps of 2 consecutive beats of an induced ventricular tachycardia in a CAR$^{+/-}$ heart show the impulse propagating around a line of block, indicating a re-entrant mechanism underlying the arrhythmia (Fig. 4C). Ventricular mRNA and protein levels of the gap junction proteins Cx43 and Cx45 were not different between WT and CAR$^{+/-}$ hearts (Figs. 5A to 5C), and there were no differences in distribution of Cx43 (in particular, no lateralization or redistribution) in ventricular cryosections (Fig. 5D) and isolated myocytes (Online Fig. 6). Protein expression levels of other intercalated disk proteins, namely β-catenin, zonula occludens 1, N-cadherin, and Cx45, were not different between WT and CAR$^{+/-}$ hearts (Online Fig. 7, Online Table 2).

Reduced sodium channel availability in CAR$^{+/-}$ mice and cardiomyocytes. Because the cardiac sodium channel protein $Na_V1.5$ is enriched in the intercalated disk region, CAR may also have an impact on conduction by affecting sodium channel expression and/or function. *Scn5a* mRNA and $Na_V1.5$ protein levels were not different between CAR$^{+/-}$ and WT ventricular tissue (Figs. 5A to 5C), and there were no differences in $Na_V1.5$ localization at the intercalated disk or lateral membrane (Fig. 5D). Functionally, however, AP upstroke velocity (dV/dtmax, a measure of sodium channel availability under near-physiological conditions [14]) was altered in cardiomyocytes isolated from CAR$^{+/-}$ hearts (Figs. 6A and 6B). On average, dV/dtmax was ≈15% lower in CAR$^{+/-}$ myocytes as compared with WT, indicating a decrease in functional sodium channel availability secondary to CAR haploinsufficiency. Resting membrane potential, AP amplitude, and AP duration were unchanged in CAR$^{+/-}$ cardiomyocytes (Fig. 6B). In vivo short-term administration of the sodium channel blocker flecainide in anesthetized mice revealed a significantly larger increase in PR interval and QRS duration in CAR$^{+/-}$ versus WT mice, underlining the functional relevance of the

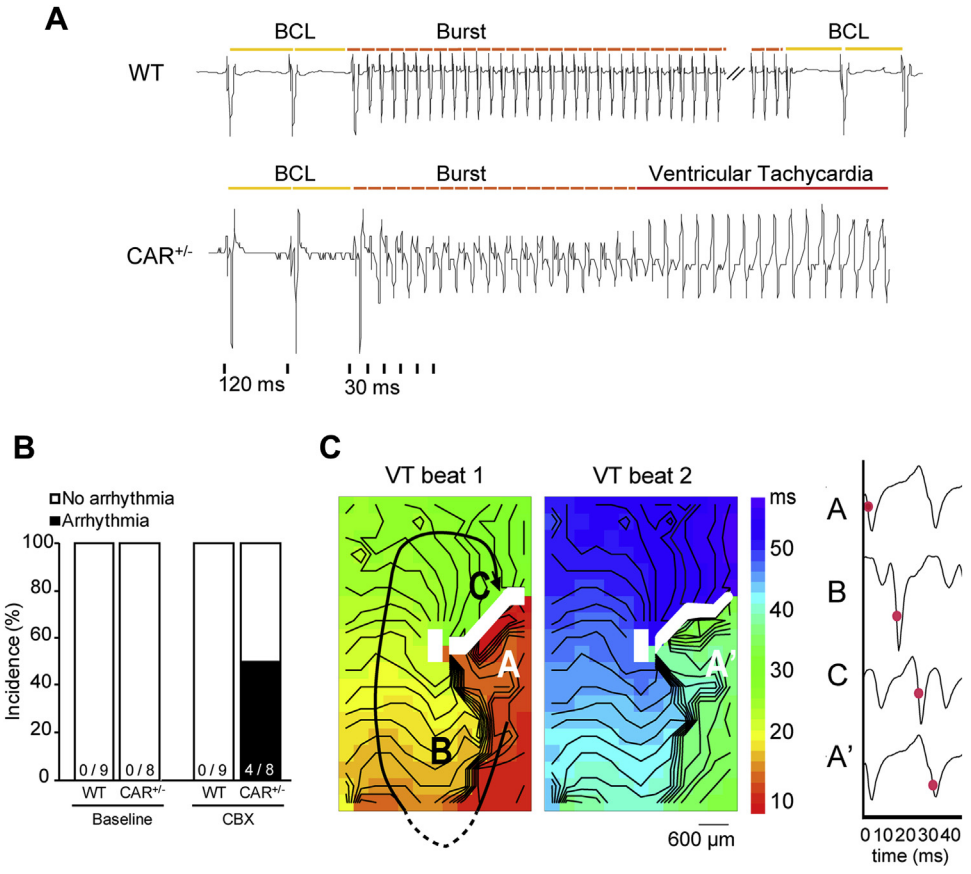

Figure 4 **Increased Arrhythmia Inducibility After Infusion of CBX in CAR$^{+/-}$ Hearts**

(A) Example of a sustained ventricular arrhythmia induced by burst pacing in a CAR$^{+/-}$ heart after infusion of CBX. **(B)** Increased incidence of inducible arrhythmias after infusion of CBX in CAR$^{+/-}$ hearts as compared with WT ($p = 0.015$). **(C)** Activation maps of 2 consecutive VT beats induced in a CAR$^{+/-}$ heart showing the impulse propagating around a line of functional conduction block, indicating a re-entrant mechanism. The **right panel** depicts electrograms at positions A, B, C, and A′ that correspond to recording sites as indicated in the activation maps **(left panel)**. Local activation times are determined as the maximal negative dV/dt in each electrogram (indicated by **red dots**). Abbreviations as in Figures 2 and 3.

reduced sodium channel availability for cardiac conduction (Online Figs. 3C and 3D).

CAR haploinsufficiency affects I_{Na} magnitude specifically at the intercalated disk. Sodium channels are located both at the lateral membrane and at the intercalated disk of the cardiomyocyte (15,16). Because CAR is localized predominantly at the intercalated disk, we hypothesized that CAR deficiency affects I_{Na} preferentially in this region. We therefore investigated I_{Na} characteristics at the lateral membrane and at the intercalated disk of isolated CAR$^{+/-}$ and WT ventricular myocytes using the macropatch cell-attached mode of the patch-clamp technique, which allows for regional assessment of I_{Na} amplitude and gating properties at a physiological temperature (36°C) (17). At the lateral membrane, the number of functional sodium channels (I_{Na} amplitude) was similar in WT and CAR$^{+/-}$ cardiomyocytes (Fig. 6C). However, a significant decrease in I_{Na} amplitude at the intercalated disk was observed in CAR$^{+/-}$ cardiomyocytes as compared with WT (Fig. 6D). Voltage dependence of I_{Na} activation and inactivation was not significantly different between WT and CAR$^{+/-}$ at the lateral membrane or at the intercalated disk (Figs. 6E and 6F). These findings indicate that CAR haploinsufficiency leads to reduced sodium channel availability secondary to a decreased I_{Na} amplitude at the intercalated disk.

Physical interaction between $Na_V1.5$ and CAR. To determine if CAR affects $Na_V1.5$ function through a physical association, we performed coimmunoprecipitation studies. FLAG-tagged human $Na_V1.5$ and/or human CAR was transiently overexpressed in HEK293 cells, and cell lysates were incubated with anti-FLAG affinity beads. Overexpressed CAR was not found to precipitate with anti-FLAG beads in the absence of $Na_V1.5$ (Fig. 7). In contrast, immunoblotting of eluates from HEK293 cells overexpressing both $Na_V1.5$ and CAR revealed that CAR coprecipitates with $Na_V1.5$ (Fig. 7), indicating a direct or indirect physical interaction between the 2 proteins.

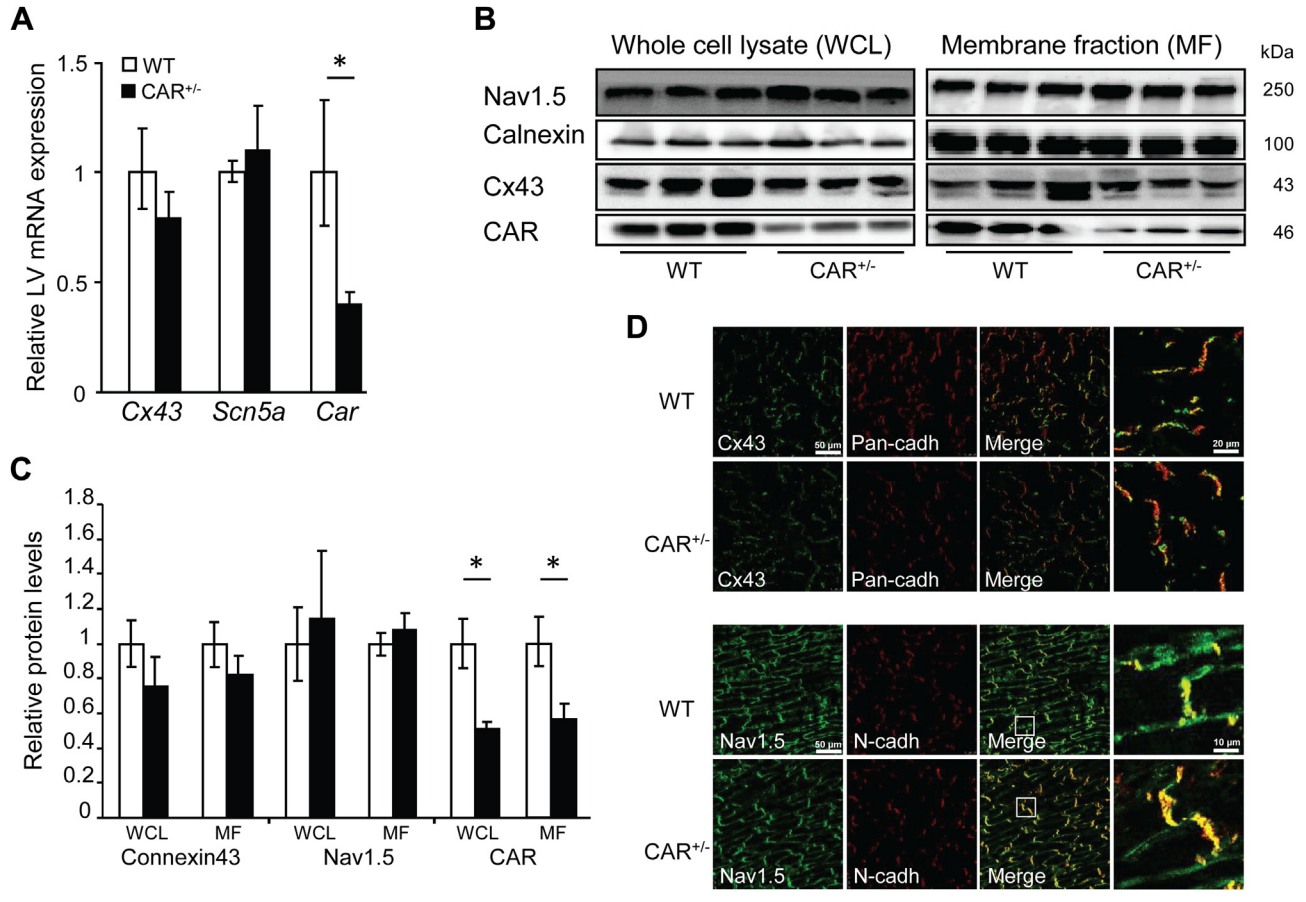

Figure 5 **Unaltered Cx43 and $Na_V1.5$ Expression and Distribution in $CAR^{+/-}$ Hearts**

(A) LV *Cx43*, *Scn5a*, and *Car* mRNA levels (n = 4 per group, *p < 0.05). **(B)** Immunoblots of $Na_V1.5$, Cx43, and CAR (whole cell and membrane fraction; calnexin as a loading control). **(C)** $Na_V1.5$, Cx43, and CAR protein levels (normalized to WT littermate control; n = 5 mice in each group; *p < 0.05). **(D)** Immunofluorescent stainings of Cx43 and $Na_V1.5$ in LV tissue; pan-cadherin (Pan-cadh) and N-cadherin (N-cadh) were used as intercalated disk markers. Cx = connexin; other abbreviations as in Figures 1 and 2.

Discussion

Our current work follows up on the discovery by a GWAS of a genetic locus on chromosome 21q21 associated with vulnerability for VF in the setting of acute MI (4). We show that in human cardiac tissue, the risk allele at this locus is associated with decreased cardiac expression of *CXADR*, suggesting that reduced levels of CAR predispose to VF during ischemia. Reduced expression of CAR in CAR haploinsufficient mice leads to slowing of ventricular conduction and earlier onset of inducible ventricular arrhythmias during acute regional myocardial ischemia, mediated (at least in part) through a reduction of I_{Na} magnitude specifically at the intercalated disk. Our findings thus establish CAR as a novel modifier of cardiac conduction and arrhythmia vulnerability in myocardial ischemia and indicate the usefulness of GWAS for the identification of novel determinants of complex phenotypes such as arrhythmia.

The rs2824292 single nucleotide polymorphism at the arrhythmia susceptibility locus on 21q21 is associated with reduced cardiac *CXADR* expression. In a recent GWAS, we identified a susceptibility locus for VF during a first acute MI at chromosome 21q21 (4). The risk haplotype at this locus, tagged by rs2824292, occurred at an intergenic region and thus likely modulates the risk of VF through effects on gene expression (18). Of the 2 genes at this locus (*CXADR* and *BTG3*), *CXADR* appears to be the most biologically plausible because previous studies have shown its myocardial localization at the intercalated disk and its modulatory effect on connexin expression and atrioventricular conduction (9,10). Our finding that carriership of the risk (G) allele at rs2824292 is associated with reduced expression of the *CXADR* gene encoding CAR in human heart samples supports the proposition that the effect of the 21q21 locus on ischemia-induced arrhythmia is mediated by CAR and suggests that decreased cardiac

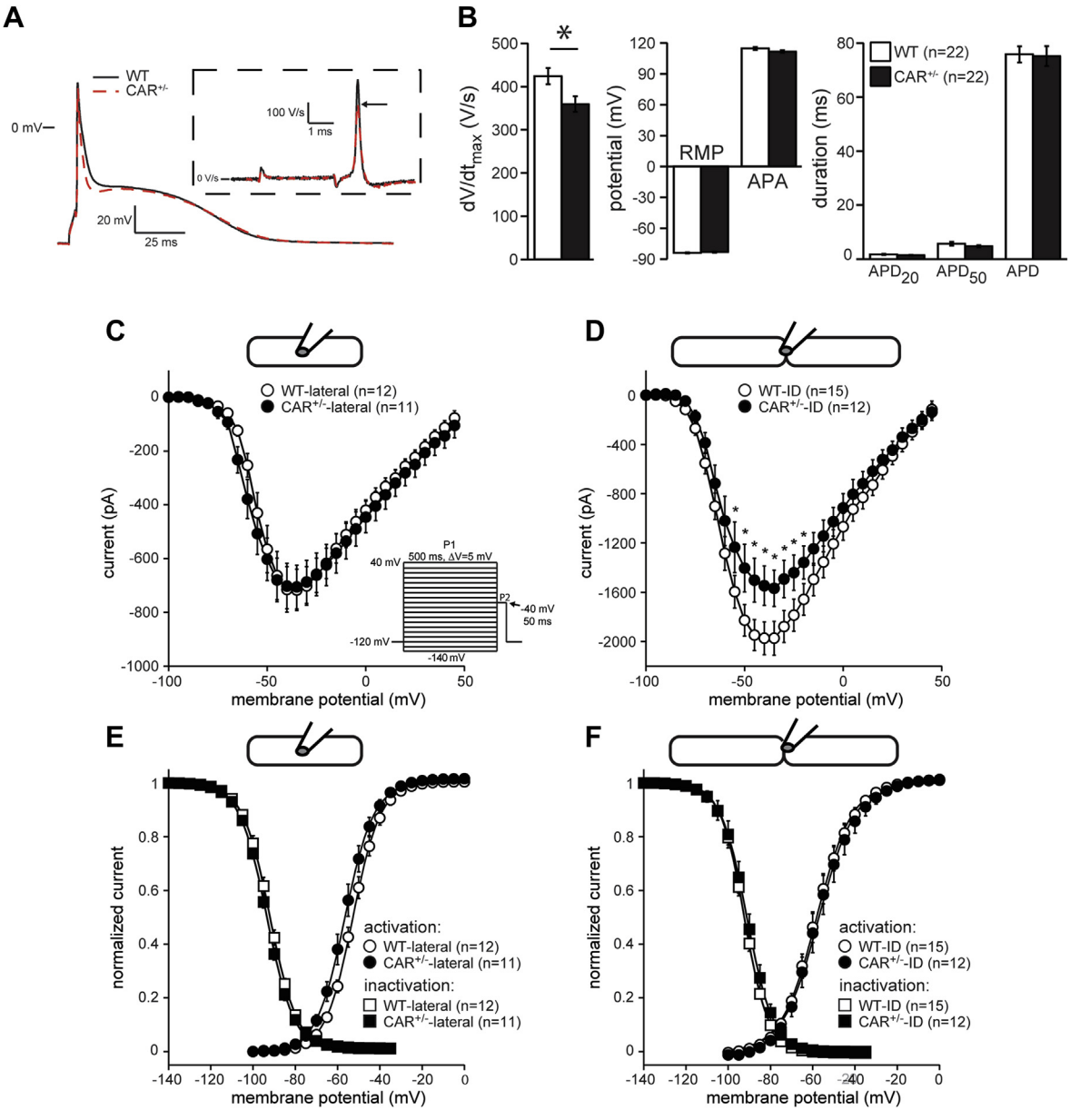

Figure 6 **Reduced Sodium Channel Availability and Decreased I_{Na} Amplitude at the Intercalated Disk in $CAR^{+/-}$ Cardiomyocytes**

(A) APs measured from isolated LV cardiomyocytes of WT and $CAR^{+/-}$ hearts (**inset**: dV/dt of the AP upstroke). **(B)** Average AP characteristics. Maximal AP upstroke velocity (dV/dtmax) was significantly lower in $CAR^{+/-}$ myocytes as compared with WT (*$p < 0.05$). Resting membrane potential, APA, and APD at 20%, 50%, and 90% of repolarization (APD_{20}, APD_{50}, and APD_{90}, respectively) were not different between WT and $CAR^{+/-}$ myocytes. **(C and D)** Current-voltage (I-V) relationships show similar I_{Na} amplitude at the lateral membrane of WT and $CAR^{+/-}$ cardiomyocytes **(C)** but reduced I_{Na} amplitude in $CAR^{+/-}$ versus WT at the intercalated disk (assessed by 2-way repeated-measures analysis of variance followed by Holm-Sidak post-hoc testing; $p = 0.002$ for overall effect) **(D)**. **Asterisks** denote membrane potentials at which I_{Na} amplitude is significantly different between WT and $CAR^{+/-}$. **(E and F)** Average voltage dependencies of activation and inactivation show no significant difference between WT and $CAR^{+/-}$ at the lateral membrane **(E)** or at the intercalated disk (ID) **(F)**. AP = action potential; APA = action potential amplitude; APD = action potential duration; I_{Na} = sodium current; RMP = resting membrane potential; other abbreviations as in Figure 2.

levels of CAR predispose to VF. The GWAS for ischemia-induced VF, which identified the chr21q21 risk locus, is thus far the only study of this specific clinical presentation. Genetic studies of this phenotype are hindered by the unavailability of large patient sets; indeed, a study by Bugert et al. (19) in a small case-control set did not detect the association of rs2824292 with VF. Thus, although the effect of the variant/haplotype that we detected on *CXADR* expression is in line with our previous GWAS findings, the robustness of this signal must be further validated in future association studies in larger patient sets.

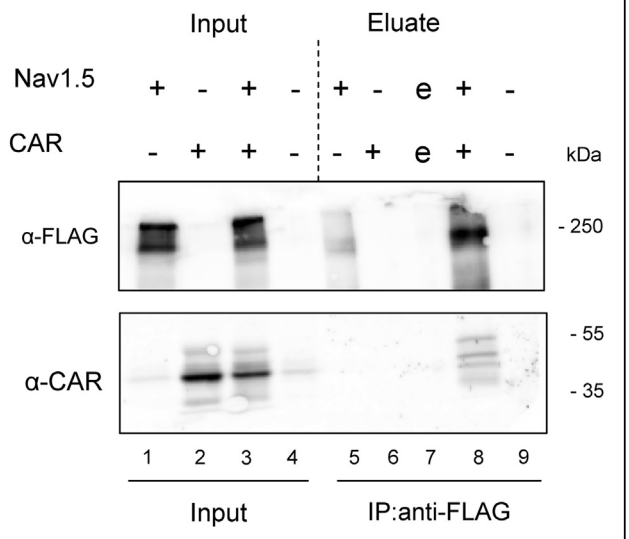

Figure 7 **CAR Interacts With $Na_V1.5$ In Vitro**

The **left panel** ("input") shows input levels of $Na_V1.5$ and CAR in lysates of HEK293A cells overexpressing FLAG-tagged $Na_V1.5$ (lane 1), CAR (lane 2), or FLAG-tagged $Na_V1.5$ together with CAR (lane 3) versus untransfected cells (lane 4). The **right panel** ("eluate") shows levels of $Na_V1.5$ and CAR after elution from FLAG-agarose beads. Neither overexpressed CAR (lane 2) nor endogenous CAR (lane 4) precipitated with anti-FLAG beads in the absence of $Na_V1.5$ (lanes 6 and 9, respectively). Eluates from HEK293 cells overexpressing both $Na_V1.5$ and CAR revealed that CAR coprecipitates with $Na_V1.5$ (lane 8). e = empty lane (lane 7). Abbreviations as in Figure 2.

Mechanism(s) of ventricular conduction slowing and arrhythmia vulnerability in $CAR^{+/-}$ mice. Conduction slowing in $CAR^{+/-}$ hearts may stem from altered cardiomyocyte excitability (i.e., sodium channel function), cell-to-cell coupling, tissue architecture, and combinations thereof. We found no evidence for myocardial hypertrophy or fibrosis in $CAR^{+/-}$ hearts, making electrical remodeling secondary to structural abnormalities unlikely. $Na_V1.5$ protein levels were unchanged in $CAR^{+/-}$ hearts, but decreased AP upstroke velocity was observed in $CAR^{+/-}$ myocytes. Moreover, prolongation of electrocardiographic conduction indexes after administration of flecainide was more pronounced in $CAR^{+/-}$ mice, further indicating the functional relevance of the reduced sodium channel availability secondary to CAR haploinsufficiency. In cardiac-specific inducible CAR knockout mice (i.e., post-natal CAR knockout mice), Cx43 protein levels in ventricular myocardium were reduced by approximately 40% (9). Although we did not detect a significant reduction of Cx43 expression in $CAR^{+/-}$ hearts, this does not preclude the possibility that subtle alterations in Cx43 expression and/or function may be of relevance for conduction, especially during perturbed conditions such as ischemia, as discussed in the following text.

Decreased membrane excitability and electrical uncoupling are key mechanisms for conduction slowing and conduction block during ischemia and provide a proarrhythmic substrate for the development of re-entrant ventricular arrhythmias (20,21). The ventricular conduction slowing in $CAR^{+/-}$ hearts likely exacerbates conduction slowing during ischemia, thereby contributing to arrhythmogenesis in this setting. The degree of conduction slowing observed at baseline in $CAR^{+/-}$ hearts was modest and not sufficient to facilitate spontaneous or induced ventricular arrhythmias. Thus, for (re-entrant) arrhythmias to occur, additional electrical and/or structural perturbations appear to be necessary, such as intercellular uncoupling or ischemia. Infusion of carbenoxolone, a gap junctional uncoupler that does not affect AP characteristics or underlying ion currents (13), further decreased conduction velocity in both the longitudinal and the transversal direction and increased arrhythmia susceptibility in $CAR^{+/-}$ but not in WT hearts. Of note, carbenoxolone also decreased conduction velocity in WT hearts, and although the magnitude of the effects of carbenoxolone was similar in both WT and $CAR^{+/-}$ hearts, the absolute values of both CVL and CVT were lowest in $CAR^{+/-}$ hearts after treatment with carbenoxolone. The concomitant reduction in sodium channel availability in $CAR^{+/-}$ hearts (but not in WT hearts) makes these hearts more susceptible to arrhythmias in the presence of the uncoupler carbenoxolone. Interestingly, an earlier onset of ventricular arrhythmias during ex vivo regional ischemia was also observed in hearts from Cx43 haploinsufficient mice (22), similar to our current observation in $CAR^{+/-}$ hearts. Because infusion of carbenoxolone is arrhythmogenic in $CAR^{+/-}$ mice, subtle alterations in gap junction proteins (undetected in our study) may contribute to the observed ischemia-induced proarrhythmia in $CAR^{+/-}$ hearts. On the other hand, arrhythmias in the early phase of ischemia are predominantly associated with conduction delay (which can facilitate re-entry) secondary to decreased membrane excitability in depolarized tissue. Thus, reduced sodium channel availability secondary to decreased I_{Na} (as shown in $CAR^{+/-}$ myocytes) may also contribute to increased arrhythmia susceptibility.

Several animal models have been developed to study CAR. Of these, the complete (germline) constitutive knockout results in early embryonic lethality characterized by severe cardiac morphological defects (23,24), cardiac-specific knockout mice develop cardiomyopathy and/or atrioventricular conduction disturbance (10), and the cardiac-specific inducible knockout develops progressive atrioventricular block (9). We chose to investigate the effects of CAR in heterozygous knockout mice to assess the impact of a less drastic reduction in CAR in the absence of remodeling, which may better reflect the variability in CAR levels occurring in human health and disease. Our observation that CAR haploinsufficiency results in ventricular conduction slowing appears to be in contrast to findings in cardiac-specific knockout hearts, in which atrioventricular conduction was abnormal but ventricular conduction velocities remained unaffected (10). However, this discrepancy may be attributed to differences in measuring techniques, targeting strategies, or genetic backgrounds (25).

CAR affects cardiac sodium channels at the intercalated disk. CAR is a cell adhesion molecule with multiple binding partners, including the scaffolding protein zonula occludens 1, which in turn interacts with Cx43 (8,26). Sodium channels interact with Cx43 and are regulated by cell adhesion molecules, including the sodium channel β-subunit and ankyrin-G (27,28). Thus, CAR may exert its effects on sodium channel availability by both direct and indirect mechanisms, which are likely not mutually exclusive. Crucially, I_{Na} was reduced at the intercalated disk of $CAR^{+/-}$ myocytes, whereas I_{Na} at the lateral myocyte membrane was unaffected. Because sodium channels at the intercalated disk are considered essential for proper conduction (15), a decrease in I_{Na} in this region is likely to impair function. Indeed, our findings show that a relatively modest reduction in I_{Na} at the intercalated disk is sufficient for sodium channel availability to be decreased. Moreover, we found that CAR interacts with $Na_V1.5$ in vitro, suggesting that CAR affects sodium channel function through a physical interaction with $Na_V1.5$. The observation that CAR affects I_{Na} specifically at the intercalated disk is in line with the emerging concept that cross talk exists between structural and electrical components in the intercalated disk region (29–31).

Study limitations. Extrapolation from studies with animal models to humans should be done with caution. We have shown increased arrhythmia inducibility in $CAR^{+/-}$ hearts after carbenoxolone and earlier onset of arrhythmia inducibility in $CAR^{+/-}$ hearts after LAD ligation but did not observe spontaneous arrhythmias in these settings. Arrhythmia-inducing triggers in patients with ischemia-induced arrhythmias may not be present in our model and vice versa, and patients may differentially compensate CAR deficiency.

Despite the observed CAR-dependent differences in AP upstroke velocity and INa at the intercalated disk, we did not detect changes in NaV1.5 protein. Nevertheless, small yet functionally relevant differences in amount and/or localization of NaV1.5 may be present, albeit below the detection limit of our Western blot and immunohistochemistry assays.

Conclusions

Our expression studies in the human heart, combined with electrophysiological studies in $CAR^{+/-}$ mice, establish a novel role for CAR in mediating ventricular conduction and arrhythmogenesis during conditions such as gap junctional uncoupling or myocardial ischemia. CAR may have similar modulatory effects on cardiac electrical activity in other pathophysiological conditions, including dilated cardiomyopathy and myocarditis, which require further investigation. The regulatory effects of CAR on sodium channel availability and cardiac conduction provide additional insight into the complex mechanisms underlying arrhythmogenesis during myocardial ischemia. Furthermore, genetic determinants of arrhythmia susceptibility during myocardial ischemia (such as CAR) may constitute future targets for risk stratification and prevention of potentially lethal ventricular arrhythmias in patients with coronary artery disease.

Acknowledgments

The authors thank Drs. J. M. Ruijter and M. W. T. Tanck for support with statistical analysis; R. Wolswinkel, L. Beekman, M. Westerveld, and B. Goldbrich for technical support; U. Wrackmeyer, U. Lisewski, M. Radke, and Y. Shi for support with animal maintenance and phenotyping; Dr. A. Varró (University of Szeged, Szeged, Hungary), Dr. C. Q. Simmons (Vanderbilt University, Nashville, Tennessee), Dr. A. Li (University of Sydney, Sydney, Australia) and Drs. T. Zhang and V. Otero (University of Miami, Miami, Florida) for assistance in obtaining and preparing human cardiac tissue samples; and Dr. H. L. Tan for critical reading of the manuscript.

Reprint requests and correspondence: Dr. Carol Ann Remme, Department of Experimental Cardiology, Heart Failure Research Center, Academic Medical Center, Room K2-104.2, Meibergdreef 15, 1105 AZ Amsterdam, the Netherlands. E-mail: c.a.remme@amc.uva.nl.

REFERENCES

1. Rubart M, Zipes DP. Mechanisms of sudden cardiac death. J Clin Invest 2005;115:2305–15.
2. Dekker LRC, Bezzina CR, Henriques JPS, et al. Familial sudden death is an important risk factor for primary ventricular fibrillation: a case-control study in acute myocardial infarction patients. Circulation 2006;114:1140–5.
3. Kaikkonen KS, Kortelainen M-L, Linna E, Huikuri HV. Family history and the risk of sudden cardiac death as a manifestation of an acute coronary event. Circulation 2006;114:1462–7.
4. Bezzina CR, Pazoki R, Bardai A, et al. Genome-wide association study identifies a susceptibility locus at 21q21 for ventricular fibrillation in acute myocardial infarction. Nat Genet 2010;42:688–91.
5. Winkler GS. The mammalian anti-proliferative BTG/Tob protein family. J Cell Physiol 2010;222:66–72.
6. Noutsias M, Fechner H, de Jonge H, et al. Human coxsackie-adenovirus receptor is colocalized with integrins αvβ3 and αvβ5 on the cardiomyocyte sarcolemma and upregulated in dilated cardiomyopathy: implications for cardiotropic viral infections. Circulation 2001;104:275–80.
7. Shaw CA, Holland PC, Sinnreich M, et al. Isoform-specific expression of the Coxsackie and adenovirus receptor (CAR) in neuromuscular junction and cardiac intercalated discs. BMC Cell Biol 2004;5:42.
8. Cohen CJ, Shieh JT, Pickles RJ, Okegawa T, Hsieh JT, Bergelson JM. The coxsackievirus and adenovirus receptor is a transmembrane component of the tight junction. Proc Natl Acad Sci U S A 2001;98:15191–6.
9. Lisewski U, Shi Y, Wrackmeyer U, et al. The tight junction protein CAR regulates cardiac conduction and cell-cell communication. J Exp Med 2008;205:2369–79.
10. Lim B, Xiong D, Dorner A, et al. Coxsackievirus and adenovirus receptor (CAR) mediates atrioventricular-node function and connexin 45 localization in the murine heart. J Clin Invest 2008;118:2758–70.
11. Fechner H, Noutsias M, Tschoepe C, et al. Induction of coxsackievirus-adenovirus-receptor expression during myocardial tissue formation and remodeling: identification of a cell-to-cell contact-dependent regulatory mechanism. Circulation 2003;107:876–82.
12. Shi Y, Chen C, Lisewski U, et al. Cardiac deletion of the Coxsackievirus-adenovirus receptor abolishes Coxsackievirus B3

infection and prevents myocarditis in vivo. J Am Coll Cardiol 2009;53:1219–26.
13. De Groot JR, Veenstra T, Verkerk AO, et al. Conduction slowing by the gap junctional uncoupler carbenoxolone. Cardiovasc Res 2003;60:288–97.
14. Berecki G, Wilders R, De Jonge B, Van Ginneken ACG, Verkerk AO. Re-evaluation of the action potential upstroke velocity as a measure of the Na^+ current in cardiac myocytes at physiological conditions. PloS One 2010;5:e15772.
15. Kucera JP, Rohr S, Rudy Y. Localization of sodium channels in intercalated disks modulates cardiac conduction. Circ Res 2002;91:1176–82.
16. Petitprez S, Zmoos A-F, Ogrodnik J, et al. SAP97 and dystrophin macromolecular complexes determine two pools of cardiac sodium channels Nav1.5 in cardiomyocytes. Circ Res 2011;108:294–304.
17. Verkerk AO, Van Ginneken ACG, Van Veen TAB, Tan HL. Effects of heart failure on brain-type Na^+ channels in rabbit ventricular myocytes. Europace 2007;9:571–7.
18. Cookson W, Liang L, Abecasis G, Moffatt M, Lathrop M. Mapping complex disease traits with global gene expression. Nat Rev Genet 2009;10:184–94.
19. Bugert P, Elmas E, Stach K, et al. No evidence for an association between the rs2824292 variant at chromosome 21q21 and ventricular fibrillation during acute myocardial infarction in a German population. Clin Chem Lab Med 2011;49:1237–9.
20. Janse MJ, Wit AL. Electrophysiological mechanisms of ventricular arrhythmias resulting from myocardial ischemia and infarction. Physiol Rev 1989;69:1049–69.
21. Coronel R, Wilms-Schopman FJ, Opthof T, Van Capelle FJ, Janse MJ. Injury current and gradients of diastolic stimulation threshold, TQ potential, and extracellular potassium concentration during acute regional ischemia in the isolated perfused pig heart. Circ Res 1991;68:1241–9.
22. Lerner DL, Yamada KA, Schuessler RB, Saffitz JE. Accelerated onset and increased incidence of ventricular arrhythmias induced by ischemia in Cx43-deficient mice. Circulation 2000;101:547–52.
23. Dorner AA, Wegmann F, Butz S, et al. Coxsackievirus-adenovirus receptor (CAR) is essential for early embryonic cardiac development. J Cell Sci 2005;118:3509–21.
24. Chen J-W, Zhou B, Yu Q-C, et al. Cardiomyocyte-specific deletion of the coxsackievirus and adenovirus receptor results in hyperplasia of the embryonic left ventricle and abnormalities of sinuatrial valves. Circ Res 2006;98:923–30.
25. Fischer R, Poller W, Schultheiss H-P, Gotthardt M. CAR-diology—a virus receptor in the healthy and diseased heart. J Mol Med (Berl) 2009;87:879–84.
26. Giepmans BN, Moolenaar WH. The gap junction protein connexin43 interacts with the second PDZ domain of the zona occludens-1 protein. Curr Biol 1998;8:931–4.
27. Malhotra JD, Thyagarajan V, Chen C, Isom LL. Tyrosine-phosphorylated and nonphosphorylated sodium channel beta1 subunits are differentially localized in cardiac myocytes. J Biol Chem 2004;279:40748–54.
28. Mohler PJ, Rivolta I, Napolitano C, et al. Nav1.5 E1053K mutation causing Brugada syndrome blocks binding to ankyrin-G and expression of Nav1.5 on the surface of cardiomyocytes. Proc Natl Acad Sci U S A 2004;101:17533–8.
29. Sato PY, Musa H, Coombs W, et al. Loss of plakophilin-2 expression leads to decreased sodium current and slower conduction velocity in cultured cardiac myocytes. Circ Res 2009;105:523–6.
30. Sato PY, Coombs W, Lin X, et al. Interactions between ankyrin-G, Plakophilin-2, and Connexin43 at the cardiac intercalated disc. Circ Res 2011;109:193–201.
31. Rizzo S, Lodder EM, Verkerk AO, et al. Intercalated disc abnormalities, reduced Na^+ current density, and conduction slowing in desmoglein-2 mutant mice prior to cardiomyopathic changes. Cardiovasc Res 2012;95:409–18.

Key Words: arrhythmia ■ ion channels ■ ischemia ■ single nucleotide polymorphism genetics ■ ventricular fibrillation.

APPENDIX

For the supplemental appendix, figures, and tables, please see the online version of this article.